Journal of Orthopaedic Translation 38 (2023) 84–97

Contents lists available at ScienceDirect

Journal of Orthopaedic Translation

journal homepage: www.journals.elsevier.com/journal-of-orthopaedic-translation

Melatonin suppresses bone marrow adiposity in ovariectomized rats by rescuing the imbalance between osteogenesis and adipogenesis through SIRT1 activation

Xiaoxiong Huang [a,b,c,1], Weikai Chen [a,c,1], Chao Gu [a,c,1], Hao Liu [a], Mingzhuang Hou [a,c], Wanjin Qin [a], Xuesong Zhu [a], Xi Chen [d,*], Tao Liu [a,**], Huilin Yang [a,c], Fan He [a,c,***]

[a] Department of Orthopaedics, The First Affiliated Hospital of Soochow University, Suzhou, 215006, China
[b] Hwa Mei Hospital, University of Chinese Academy of Sciences (Ningbo No. 2 Hospital), No. 41 Northwest Street, Ningbo, 315010, Zhejiang, China
[c] Orthopaedic Institute, Medical College, Soochow University, Suzhou, 215000, China
[d] Department of Pathology, The Third Affiliated Hospital of Soochow University, Changzhou, 213003, China

ARTICLE INFO

Keywords:
Melatonin
Osteogenesis
Bone marrow-derived mesenchymal stem cells
Adipogenesis
SIRT1
Marrow adiposity

ABSTRACT

Introduction: Accelerated imbalance between bone formation and bone resorption is associated with bone loss in postmenopausal osteoporosis. Studies have shown that this loss is accompanied by an increase in bone marrow adiposity. Melatonin was shown to improve impaired bone formation capacity of bone marrow-derived mesenchymal stem cells from ovariectomized rats (OVX-BMMSCs).

Objectives: To investigate whether the anti-osteoporosis effect of melatonin involves regulation of the equilibrium between osteogenic and adipogenic differentiation of osteoporotic BMMSCs.

Methods: To induce osteoporosis, female Sprague–Dawley rats received ovariectomy (OVX). Primary BMMSCs were isolated from tibiae and femurs of OVX and sham-op rats and were induced towards osteogenic or adipogenic differentiation. Matrix mineralization was determined by Alizarin Red S (ARS) and lipid formation was evaluated by Oil Red O. OVX rats were injected with melatonin through the tail vein. Bone microarchitecture was determined using micro computed tomography and marrow adiposity were examined by histology staining.

Results: OVX-BMMSCs exhibited a compromised osteogenic potential and an enhanced lineage differentiation towards adipocytes. *In vitro* melatonin improved osteogenic differentiation of OVX-BMMSCs and promoted matrix mineralization by enhancing the expression of transcription factor RUNX2 in a dose-dependent manner. Moreover, melatonin significantly inhibited lipid formation and suppressed OVX-BMMSCs adipogenesis by down-regulating peroxisome proliferator-activated receptor γ (PPARγ). Intravenous injection of melatonin prevented bone mass reduction and bone architecture destruction in ovariectomized rats. Importantly, there was a significant inhibition of adipose tissue formation in the bone marrow. Mechanistic investigations revealed that SIRT1 was involved in melatonin-mediated determination of stem cell fate. Inhibition of SIRT1 abolished the protective effects of melatonin on bone formation by inducing BMMSCs towards adipocyte differentiation.

Conclusions: Melatonin reversed the differentiation switch of OVX-BMMSCs from osteogenesis to adipogenesis by activating the SIRT1 signaling pathway. Restoration of stem cell lineage commitment by melatonin prevented marrow adipose tissue over-accumulation and protected from bone loss in postmenopausal osteoporosis.

The translational potential of this article: Determination of stem cell fate towards osteoblasts or adipocytes plays a pivotal role in regulating bone metabolism. This study demonstrates the protective effect of melatonin on bone mass in estrogen-deficient rats by suppressing adipose tissue accumulation in the bone marrow. Melatonin may serve as a promising candidate for the treatment of osteoporosis in clinics.

* Corresponding author. Department of Pathology, The Third Affiliated Hospital of Soochow University, No.185 Juqian Road, Changzhou, 213003, Jiangsu, China.
** Corresponding author. Department of Orthopaedics, The First Affiliated Hospital of Soochow University, No. 899 Pinghai Road, Suzhou, 215006, Jiangsu, China.
*** Corresponding author. Orthopaedic Institute, Soochow University, Suzhou 215000, China
E-mail addresses: chenxi1124@suda.edu.cn (X. Chen), liutao8250@suda.edu.cn (T. Liu), fanhe@suda.edu.cn (F. He).
[1] These authors contributed equally to this work.

https://doi.org/10.1016/j.jot.2022.10.002
Received 18 March 2022; Received in revised form 17 September 2022; Accepted 6 October 2022

1. Introduction

Osteoporosis, characterized by low bone mass and bone microarchitecture deterioration, is a prevalent skeletal disorder that is also an important global public health problem. Multiple factors, such as aging, estrogen withdrawal, long-term glucocorticoid use, and alcohol abuse among others are associated with the development of osteoporosis [1]. Primary osteoporosis refers to postmenopausal osteoporosis that is associated with decreased estrogen levels, and senile osteoporosis that is associated with aging [2]. The disruption in bone remodeling, in which osteoclast-mediated bone resorption process is faster than osteoblast-mediated bone formation, has been proven to induce the pathogenesis of primary osteoporosis. Current anti-osteoporosis strategies, such as calcitonin, bisphosphonates and monoclonal antibodies (e.g. denosumab), focus on osteoclasts to inhibit bone resorption [3]. These therapeutic options can only slow down osteoporosis progression and cannot reverse its pathogenesis. Recombinant human parathyroid hormone teriparatide (rhPTH 1–34) is a prevailing bone catabolic agent that can promote bone formation. However, several side effects, such as post-dose hypercalcaemia, risk of tumor formation, and cardiovascular complications limit its continued use [4]. Therefore, it is necessary to develop safer and more effective strategies for promoting bone formation in osteoporosis patients.

Bone resorption is a major contributor to bone mass reduction and is accompanied by increased marrow adiposity. Bone marrow-derived mesenchymal stem cells (BMMSCs) are the major sources of osteoblasts and they can also differentiate into adipocytes, chondrocytes, and muscle cells upon specific stimulation [5]. Determination of stem cell fate towards osteoblasts or adipocytes plays a pivotal role in regulating bone metabolism. In senile osteoporosis, there is a significant reduction in bone formation and a remarkable increase in adipose tissue formation in the bone marrow. Increased marrow adiposity is attributed to the shift from osteogenic to adipogenic differentiation of BMMSCs. Singh et al. found that transplantation of young BMMSCs into old mice retained a strong differentiation preference for adipogenesis rather than osteogenesis, implying that age-related microenvironmental alterations are responsible for imbalanced lineage commitment [6]. Several important transcriptional factors have been implicated in determination of stem cell lineage fate. Among them, RUNX2 is a crucial factor regulating stem cell osteogenesis, whereas peroxisome proliferator-activated receptor γ (PPRAγ) promotes adipocyte-related genes expression. Sui et al. isolated BMMSCs from naturally aging and accelerated senescence (SAMP6) mice and demonstrated a shift from osteogenesis to adipogenesis, accompanied by suppressed RUNX2 expression levels and up-regulated PPARγ levels [7].

Melatonin, a neurohormone synthesized in the pineal gland, plays an important role in bone homeostasis regulation [8]. Melatonin has been shown to enhance bone formation and, consequently, prevents bone loss in osteoporosis patients [9]. Igarashi-Migitaka et al. reported that orally administered melatonin successfully increased bone strength and bone mass in naturally aged mice [10]. In contrast, withdrawal of melatonin through pinealectomy in sheep led to a significant reduction in bone mass, accompanied by an increase in bone resorption [11]. Moreover, the results of two randomized trials showed that melatonin supplementation significantly increase BMD of the femoral neck in osteoporotic women [12], and it restored the imbalance in bone remodeling in healthy perimenopausal women [13]. At pharmacological concentrations, melatonin inhibited osteoclast differentiation by attenuating intracellular reactive oxygen species (ROS) [14]. Ikegame et al. confirmed the inhibitory effects of melatonin on osteoclast activation during space flight by suppressing the expression of receptor activator of nuclear factor κB ligand (RANKL) in goldfish [15].

Regarding bone formation, melatonin increases matrix mineralization by promoting the differentiation of adult MSCs into osteoblasts through the extracellular signal-regulated kinases (ERK) 1/2 signaling cascade [16]. In addition, melatonin protects MSCs from apoptosis and preserves the capacity for osteogenic differentiation even in the presence of pro-inflammatory cytokines such asIL-1β [17] and TNF-α [18]. However, the effect of melatonin on adipogenic differentiation has not been elucidated. Zhang et al. reported that melatonin inhibits adipogenic differentiation of MSCs by suppressing PPARγ expression [19], whereas Kato et al. documented that melatonin promotes adipogenic differentiation of 3T3-L1 embryo fibroblasts by up-regulating PPARγ expression and promoting mitochondrial biogenesis [20]. Therefore, it is necessary to investigate the effect of melatonin on the balance between osteogenesis and adipogenesis of BMMSCs during postmenopausal osteoporosis.

SIRT1 is a member of the sirtuin protein family and well known as a longevity gene, regulates energy metabolism, response to oxidative stress, cell survival and differentiation [21]. Importantly, SIRT1 is a potential target for treating osteoporosis, because overexpression of SIRT1 in mandibular mesenchymal stems cells elevated alveolar bone volume in Sirt1 transgenic mice (Sirt1TG) [22], while its knockout reducted cortical bone thickness and trabecular volume [23]. Tseng et al. reported that SIRT1 activation by resveratrol enhanced FOXO 3 A-dependent transcriptional activity and, subsequently, up-regulated RUNX2 expression to promote osteogenic differentiation of human MSCs [24]. Our previous studies revealed that melatonin prevented stem cell premature senescence [25] and rescued titanium nanoparticle-impaired osteogenic capacity of BMMSCs via activation of SIRT1 [26]. However, it has not been established whether the SIRT1-related signaling pathway is involved in determination of stem cell lineage fate by melatonin.

In this study, we hypothesized that melatonin prevents bone marrow adiposity by reversing stem cell imbalance between osteogenesis and adipogenesis in postmenopausal osteoporosis. BMMSCs were isolated from ovariectomized rats (OVX-BMMSCs) and induced towards osteogenic or adipogenic differentiation in the presence of melatonin. OVX rats were injected with melatonin through the tail vein, and after three months, bone microarchitecture and marrow adiposity were examined. Involvement of SIRT1 in melatonin-mediated regulation of stem cell lineage fate was also investigated.

2. Materials and methods

2.1. Animals and ovariectomy

A total of 52 eight-week-old (178.4 ± 12.4 g) female Sprague–Dawley (SD) rats were provided by the animal center of Soochow University. All the rats were kept in cages under controlled conditions (pathogen-free, 24 °C, 50% humidity) with free access to appropriate diet and water. Ovaries were surgically removed in half of rats as previously described [27]. After anesthetization (pentobarbital, 30 mg/kg, intraperitoneal injection, Yuanye, Shanghai, China), the ovaries from both sides were exposed and excised. Similar operations were performed in the sham rats except that ovaries were left intact. All the animals were sutured and injected with penicillin for three days (80,000 Units/rat, intramuscularly, Yuanye) after surgery. To isolate BMMSCs from OVX rats, three months after the surgery, twenty sham and OVX rats were euthanized for cell isolation for *in vitro* experiments. For *in vivo* experiments, one week following ovariectomy surgery, thirty-two sham and OVX rats were administrated with melatonin for three months.

2.2. Ethics statement

All experiments involving animals were conducted according to the ethical policies and procedures approved by the ethics committee of Soochow University (Approval no. SUDA20210531A01).

2.3. Isolation of BMMSCs and cell culture

Primary BMMSCs were isolated from the tibiae and femurs of OVX- or Sham-operated rats according to a previously published protocol [28].

Cells were cultured in alpha minimum essential medium (α-MEM) containing 10% fetal bovine serum (FBS) and 1% penicillin-streptomycin (all from Thermo Fisher Scientific, Waltham, MA) in a 37 °C incubator with a 5% CO_2 atmosphere. All the BMMSCs were passaged at 90% confluence by being treated with 0.25% trypsin.

2.4. Treatments with melatonin and sirtinol

Melatonin (Sigma–Aldrich) was dissolved in absolute alcohol (EtOH) to achieve a storage solution at the concentration of 250 mM. For *in vitro* experiments, melatonin solution was diluted to 1 μM or 100 μM with the culture medium, while an equal volume of α-MEM containing 0.04% ethanol was used in the vehicle (EtOH) group. To inhibit SIRT1 activity, 40 μM of sirtinol (Sigma–Aldrich), along with 100 μM of melatonin was supplemented in the culture medium.

2.5. Cell viability and proliferation assays

The cell viability and proliferation of BMMSCs was determined with CCK-8 assay (Beyotime, Shanghai, China). To assess cell viability, BMMSCs were seeded on a 96-well plate at the density of 10,000 cells/well and after 48 h, working solution of CCK-8 (100 μL per well) was added and was then incubated at dark 37 °C in 5% CO_2 for 2 h. To assess cell proliferation, BMMSCs were seeded on a 96-well plate at the density of 1000 cells/well. At days 1, 3, 5 and 7, working solution was added and was then incubated at dark. The optical density at 450 nm wavelength was read by a multifunctional microplate reader (BioTek, Winooski, USA). Cell morphologies were observed by a microscope (Olympus, Tokyo, Japan).

2.6. Osteogenic differentiation of BMMSCs

To induce osteogenic differentiation, BMMSCs in a 12-well plate were incubated in osteogenic induction medium (α-MEM containing 10% FBS, 100 nM dexamethasone, 10 mM β-glycerol phosphate, 50 μg/mL L-ascorbic acid and 1% penicillin-streptomycin). After two weeks, differentiated cells would be fixed by 4% paraformaldehyde for 15 min. After fixation, 0.1% alizarin red S (ARS) solution (Sigma–Aldrich) was added to each well for 20 min. An Olympus IX51 microscope was used to take a picture of stained matrices. For mineralization quantification, the stain was dissolved by 5% perchloric acid solution (Sigma–Aldrich) for 30 min, followed by measurement of absorbance at 420 nm using a spectrophotometer.

2.7. Adipogenic differentiation of BMMSCs

Adipogenic differentiation of BMMSCs was induced for 14 days using a Mesenchymal Stem Cell Adipogenic Differentiation Kit according to the manufacture's protocol (RASMD-90031, Cyagen, Guangzhou, China) [28]. Adipocyte formation was assessed with Oil Red O (Sigma–Aldrich) staining method. After fixation of the differentiated cells, oil red O working solution was added in each well for 30 min. An Olympus IX51 microscope was used to take a picture of stained fat droplets in the adipocytes. For quantification, isopropanol was used to dissolve the stained fat droplets and absorbance at 510 nm was spectrophotometrically.

2.8. Quantitative analysis of RT-PCR

The TRIzol® reagent (Thermo Fisher Scientific) was used to isolate RNA of all the cells. Afterwards, total RNA (1 μg) was reverse-transcribed into cDNA. Quantitative RT-PCR reaction was performed on a CFX96TM PCR system (Bio-Rad). All the primer sequences were presented in Table 1. Differences in gene expression were analyzed by the comparative Ct ($2^{-\Delta\Delta Ct}$) method after normalizing by the *Gapdh* gene.

Table 1
Primers used for quantitative real-time polymerase chain reaction (RT-PCR).

Gene	Forward Primer sequence(5′-3′)	Reverse Primer sequence(5′-3′)
Sirt1	GAAAATGCTGGCCTAATAGACTTG	TGGTACAAACAAGTATTGATTACCG
Runx2	CCAACTTCCTGTGCTCCGTG	GTGAAACTCTTGCCTCGTCCG
Sp7	CCCAACTGTCAGGAGCTAGAG	GATGTGGCGGCTGTGAAT
Bglap	GACCCTCTCTCTGCTCACTCT	GACCTTACTGCCCTCCTGCTTG
Pparg	CCTATTGACCCAGAAAGCGATT	CATTACGGAGAGATCCACGGA
Lpl	ACAAGAGAGAACCAGACTCCAA	AGGGTAGTTAAACTCCTCCTCC
Fabp4	AACCTTAGATGGGGGTGTCCTG	TCGTGGAAGTGACGCCTTTC
Gapdh	GCAAGTTCAACGGCACAG	CGCCAGTAGACTCCACGAC

2.9. Western blot

All protein expression was measured by Western blot. Briefly, 20 μg of protein for each sample were denatured at 100 °C for 5–10 min and separated on 10% SDS-PAGE. The proteins were eletrophoretically transferred onto nitrocellulose membranes (Beyotime, Shanghai, China). After being blocked, the blots were incubated overnight using primary antibodies at 4 °C. All the primary antibodies used were provided by Abcam: anti-SIRT1 (1:5000, ab189494), anti-RUNX2 (1:2000, ab76956), anti-PPARγ (1:2000, ab272718) and anti-α Tubulin (1:10000, ab7291). Afterwards, the blots were incubated using secondary antibodies (1:10000, ab6721 or ab6789) at RT for 1 h. The blots were detected with the chemiluminescence reagent (Thermo Fisher Scientific). The ImageJ software (NIH, Bethesda, MD) was used to measure all band intensities.

2.10. In vivo administration of melatonin

Melatonin was dissolved in absolute EtOH and further diluted in saline (0.9% NaCl) to give a final concentration of 5 mg/mL (containing 10% EtOH). One week following ovariectomy surgery, thirty-two sham and OVX rats were randomly assigned to four groups: sham, sham + MT, OVX, and OVX + MT. The rats were injected with melatonin solution (10 mg/kg) via the tail vein twice per week for 3 months according to a previously published protocol [27]. Other rats that had not been assigned to melatonin treatment were administered with the same amount of ethanol through the tail vein. Melatonin was injected during 10:00–10:30 AM daily with an infusion of about 5 s per rat to avoid possible physiological interference.

2.11. Micro computed tomography (μCT) analysis

Rats were euthanized with diethyl ether 3 days after the last melatonin administration. The entire femur of the rat was isolated and distal portion of femur tissue samples were evaluated using a high resolution Skyscan 1176 system (Bruker, Aartselaar, Belgium) at a spatial resolution of 9 μm (65 kV, 385 μA, 200 ms integration time) as previously described [27]. No. 51 to 150 cancellous bone sections below the top of epiphyseal line were chosen as the region of interest. Cancellous bone morphometric data from 3D reconstructed images of the region of interest containing bone mineral density (BMD, g/cm^3), bone volume ratio (BV/TV, %) and trabecular separation (Tb.Sp, mm) were calculated using a micro-CT analysis software according to international guidelines [29].

2.12. Histological staining and in vivo oil red O staining

After μCT scanning, femurs for histological staining were decalcified in 10% EDTA for 6 weeks. After that, embedded femur specimens were cut into 9-μm-thick sections by a paraffin microtome. The obtained section were subjected to hematoxylin and eosin (H&E) staining.

To evaluate the adipose tissue in bone marrow, frozen sections were stained by Oil red O solution. Femur specimens were equilibrated in 15% and 30% sucrose each for 24 h. The sucrose-penetrated samples were subsequently covered with optimal cutting temperature (OCT) compound and snap-frozen. Frozen blocks were cut into 9-μm-thick sections

using a Leica CM3050S cryostat (Leica Microsystems, Nussloch, Germany). The obtained frozen section were pre-treated by 60% isopropanol for 10 min, stained with 3% Oil Red O solution for 15 min, and counterstained in hematoxylin for 1 min. Image acquisition was performed on an Axiovert 200 microscope (Zeiss, Oberkochen, Germany).

2.13. Statistics

After passing Shapiro–Wilk normality test, all the results were presented as mean ± standard deviation (S.D.). Differences between 2 groups were analyzed using Student's *t*-test and more than 2 comparisons were conducted by one-way analysis of variance (ANOVA) followed by Tukey's HSD post-hoc test. Differences were proved statistically significant if $p \leq 0.05$ (*) or highly significant if $p \leq 0.01$ (**). All the analysis was performed by SPSS 14.0 software (SPSS Inc., Chicago, USA).

3. Results

3.1. OVX-BMMSCs exhibited lineage commitment towards adipocytes rather than osteoblasts

BMMSCs isolated from Sham and OVX rats exhibited similar cell morphologies (Fig. 1A), while cell proliferation levels of OVX-BMMSCs were significantly lower than those from the sham group (Fig. 1B). Due to the important role of SIRT1 in regulating stem cell lineage differentiation, we evaluated the expression of SIRT1 in BMMSCs. Transcript levels of *Sirt1* in OVX-BMMSCs were 55.8% lower than those of the sham group (Fig. 1C). Protein expression of SIRT1 in OVX-BMMSCs was 26.3% lower than that of the Sham group. RUNX2 and PPARγ are two critical transcription factors that determine stem cell fate. In OVX-BMMSCs, protein levels of RUNX2 were 25.9% low while those of PPARγ were 36.0% higher when compared to sham cells (Fig. 1D&E), suggesting that OVX-BMMSCs had a lineage preference for adipocyte differentiation.

Next, we examined differences in lineage-specific differentiation in both cells. OVX-BMMSCs exhibited a weak osteogenic differentiation ability. The level of matrix mineralization of OVX-BMMSCs was 85.0% lower than that of the Sham group (Fig. 1F). Consistently, expression of osteoblast-specific markers, containing *Runx2*, *Sp7* (osterix) and *Bglap* (osteocalcin) were significantly suppressed in the OVX group (Fig. 1G). Following adipogenic induction, lipid formation in the OVX group was 2.6-fold more than that in the Sham group (Fig. 1H), while gene expression levels of adipocyte-specific markers, including *Lpl*, *Pparg* and *Fabp4* exhibited similar elevated levels, implying that OVX-BMMSCs had an enhanced adipogenic potential and a compromised osteogenic differentiation (Fig. 1I).

In vitro treatments with melatonin restored differentiation equilibrium between osteogenesis and adipogenesis for OVX-BMMSCs.

OVX-BMMSCs were treated with 1 or 100 μM melatonin. Cell viability assay showed that melatonin treatment even at 100 μM had no cytotoxic effect on BMMSCs (Supplementary Fig. 1A). Cell morphologies of OVX-BMMSCs were not altered in the presence of melatonin, while cell densities of melatonin-treated cells were higher than those of the controls (Fig. 2A). Consistently, CCK-8 analysis revealed that melatonin significantly improved cell proliferation levels of OVX-BMMSCs. At day 7, melatonin was found to have enhanced cell proliferation by 27.7% at 1 μM and by 51.1% at 100 μM, respectively (Fig. 2B). Compared to controls, gene expression levels of *Sirt1* in melatonin-treated cells were found to have been up-regulated by 32.8% at 1 μM and by 92.7% at 100 μM, respectively (Fig. 2C). Western blot assays confirmed that melatonin treatment significantly elevated SIRT1 protein expression in OVX-BMMSCs in a dose-dependent manner. Interestingly, protein expression levels of RUNX2 were up-regulated by 87.8% in the presence of 100 μM melatonin, while PPARγ expression levels were down-regulated by 28.8% (Fig. 2D&E). These results indicate that melatonin reverses lineage commitment of OVX-BMMSCs toward osteogenesis.

We further investigated whether melatonin restored differentiation equilibrium between osteogenesis and adipogenesis for OVX-BMMSCs. ARS staining revealed that melatonin significantly enhanced calcium deposition in a dose-dependent manner. Compared to the control group, matrix mineralization levels were increased 1.2-fold and 2.7-fold after 1 and 100 μM melatonin treatments, respectively (Fig. 2F&G). Transcript levels of osteoblast-specific markers were also found to have been up-regulated by melatonin. In particular, mRNA expression levels of *Bglap* exhibited a 1.2-fold and 3.6-fold increase after 1 and 100 μM melatonin treatments, respectively (Supplementary Fig. 1B). Oil red O staining revealed that melatonin suppressed OVX-BMMSCs differentiation towards adipocytes. Compared to the controls, levels of mature lipids were suppressed by 46.5% and 70.3% in the presence of 1 and 100 μM melatonin, respectively (Fig. 2H&I). Accordingly, gene expression levels of adipocyte-specific markers were significantly down-regulated by melatonin. For example, compared to the control group, treatment with 100 μM melatonin inhibited gene expression of *Lpl* by 61.8%, *Pparg* by 55.5% and *Fabp4* by 55.7% (Supplementary Fig. 1C).

Inhibition of SIRT1 expression abrogated the effects of melatonin on the differentiation balance of OVX-BMMSCs.

To establish the potential role of SIRT1 in regulating stem cell fate, OVX-BMMSCs were treated with sirtinol to inhibit SIRT1 activity in the presence of 100 μM melatonin. Compared to the MT group, cell proliferation levels of sirtinol-treated cells were significantly decreased by 30.3% (Fig. 3A&B). Treatment with sirtinol suppressed the gene and protein expression of SIRT1 by 37.0% (Figs. 3C) and 29.2% (Fig. 3D), respectively. Protein expression levels of RUNX2 were suppressed by 40.4%, while those of PPARγ were elevated by 57.2% after sirtinol treatment (Fig. 3D&E).

After osteogenic induction, matrix mineralization in sirtinol-treated OVX-BMMSCs was decreased by 70.8% compared to the MT group (Fig. 3F&G). Consistently, compared to the melatonin-treated cells, sirtinol treatment down-regulated mRNA expression levels of *Runx2* by 37.3%, *Sp7* by 80.9% and *Bglap* by 88.2% (Supplementary Fig. 2A). Moreover, sirtinol treatment improved adipogenic differentiation of OVX-BMMSCs. Compared to the MT group, lipid formation levels were increased 2.3-fold in sirtinol-treated cells (Fig. 3H&I). Sirtinol significantly up-regulated mRNA expression levels of *Lpl* by 1.9-fold, *Pparg* by 82.5% and *Fabp4* by 1.3-fold compared to the MT group (Supplementary Fig. 2B). These findings show that inhibition of SIRT1 by sirtinol suppressed the advantages of melatonin on osteogenesis, while stimulating adipogenic differentiation of OVX-BMMSCs.

Melatonin treatment protected against OVX-induced bone loss by suppressing adipose tissue accumulation in the bone marrow.

To determine the protective effects of melatonin against estrogen deficiency-induced bone loss, sham and OVX rats were treated with melatonin (10 mg/kg) through the tail vein for three months. In OVX rats, estrogen deficiency was associated with less trabecular bone in distal femur. However, melatonin injection protected trabecular microarchitecture structure and preserved bone mass (Fig. 4A). Three-dimensional (3D) reconstruction analysis revealed that, compared to their controls, BMD and BV/TV of OVX rats were significantly decreased by 47.6% and 60.0%, respectively. However, compared to the OVX group, melatonin treatment significantly improved BMD by 44.7% and BV/TV by 73.6% (Fig. 4B&C). In contrast, Tb.Sp in the OVX group was increased by 67.4%, whereas melatonin treatment down-regulated it by 22.2% (Fig. 4D).

Histology revealed a significant bone loss in OVX rats, while melatonin administration protected trabecular bone microarchitecture in the OVX rats (Fig. 4E). To observe changes in osteogenic and adipogenic lineage differentiation *in vivo*, we evaluated adipocyte formation in the bone marrow of sham and OVX rats (Fig. 4F). There was an increased abundance of adipose tissues in the bone marrow milieu of OVX rats, accompanied by bone loss. Oil red O staining proved that the number of adipocytes and fatty marrow area in OVX rats were significantly increased by 28.8-fold and 27.1-fold, respectively, implying that estrogen deficiency resulted in a lineage differentiation disorder in OVX rats.

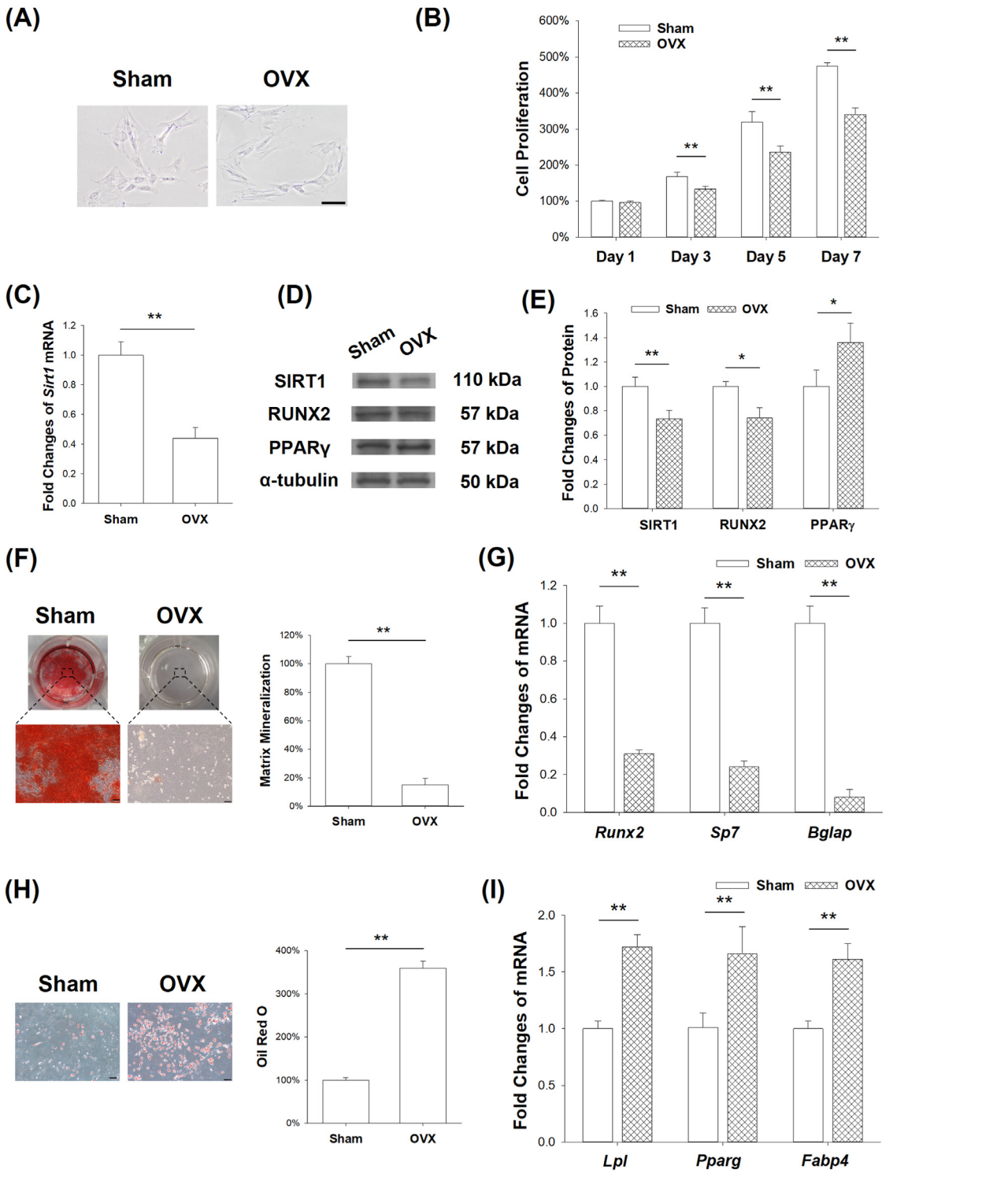

Fig. 1. BMMSCs from ovariectomized rats (OVX-BMMSCs) exhibited impaired osteogenic potential and enhanced adipogenic differentiation ability (A) BMMSCs from Sham and OVX rats exhibited similar cell morphologies. Scale bar, 100 μm. Magnificantion, 100X. (B) Proliferation of Sham- and OVX-BMMSCs (C) Gene expression of Sirt1. (D–E) Protein expression of SIRT1, RUNX2 and PPARγ (F) Representative images and quantitative analysis of ARS staining that was conducted to evaluate matrix mineralization. Scale bar, 100 μm. Magnificantion, 100X. (G) Osteoblast-related gene expression: Runx2, Sp7 and Bglap (H) BMMSCs were induced towards adipogenesis for 14 days and stained by oil red O. Representative images and quantitative analysis were used to examine lipid formation in mature adipocytes. Scale bar, 100 μm. Magnificantion, 100X. (I) Adipocyte-specific gene expression: Lpl, Pparg and Fabp4. Values are the mean ± S.E.M of six independent experiments (n = 6) in cell proliferation assays, four independent experiments (n = 4) in RT-PCR experiments, ARS assays, and Oil Red O staining assays, and three independent experiments (n = 3) in Western blot assays. Statistically significant differences are indicated by * where $p < 0.05$ or ** where $p < 0.01$ between the indicated groups.
Abbreviations: BMMSCs, bone marrow mesenchyml stem cells; OVX, ovariectomized; SIRT1, Silent information regulator type 1; RUNX2, runt-related transcription factor 2; Sp7, osterix; Bglap, bone gamma carboxyglutamate protein; PPARγ, peroxisome proliferator-activated receptor γ; Fabp4, fatty acid binding protein 4; LPL, lipoprotein lipase.

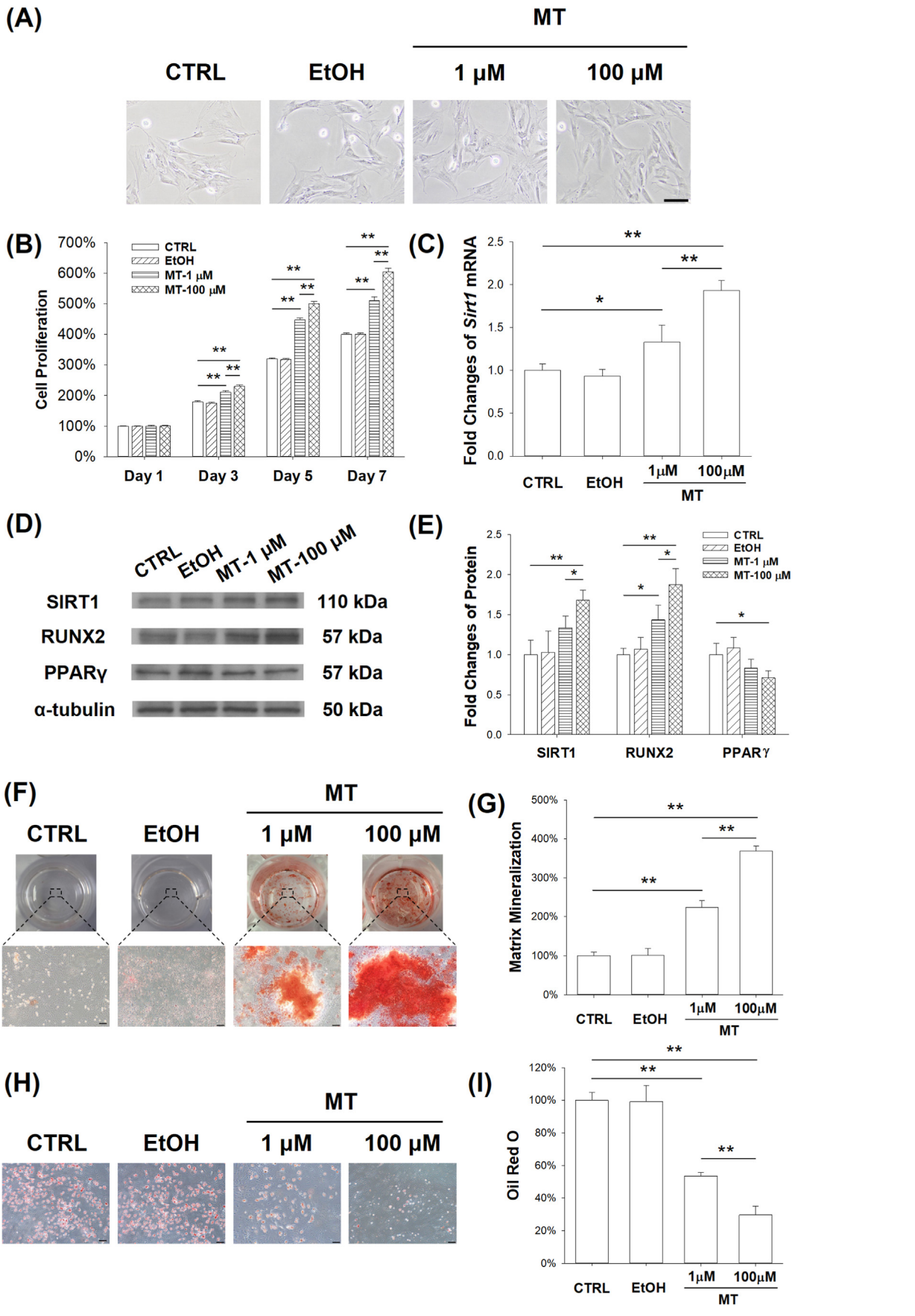

(caption on next page)

Fig. 2. Effects of melatonin on cell proliferation and lineage commitment of OVX-BMMSCs (A) Melatonin treatments (1 or 100 μM) did not alter cell morphologies of OVX-BMMSCs. Scale bar, 100 μm. Magnificantion, 100X (B) Proliferation levels of OVX-BMMSCs were significantly elevated by melatonin. (C) Gene expression of Sirt1 (D–E) Protein expression levels of SIRT1, RUNX2 and PPARγ. (F–G) Representative images and quantitative analysis of ARS staining that was conducted to evaluate matrix mineralization in the presence of 1 or 100 μM melatonin. Scale bar, 100 μm. Magnificantion, 100X (H–I) Lipid formation in mature adipocytes in the presence of 1 or 100 μM melatonin were determined by oil red O staining. Scale bar, 100 μm. Magnificantion, 100X. Values are the mean ± S.E.M of six independent experiments (n = 6) in cell proliferation assays, four independent experiments (n = 4) in RT-PCR experiments, ARS assays, and Oil Red O staining assays, and three independent experiments (n = 3) in Western blot assays. Statistically significant differences are indicated by * where $p < 0.05$ or ** where $p < 0.01$ between the indicated groups.
Abbreviations: MT, melatonin; EtOH, ethyl alcohol; SIRT1, Silent information regulator type 1; RUNX2, runt-related transcription factor 2; Sp7, osterix; Bglap, bone gamma carboxyglutamate protein; PPARγ, peroxisome proliferator-activated receptor γ; Fabp4, fatty acid binding protein 4; LPL, lipoprotein lipase.

However, after melatonin treatment, the number of adipocytes in the OVX rat bone marrow was reduced by 88.6% (Fig. 4G) while the fatty marrow area was decreased 94.2% (Fig. 4H). These findings suggest that intravenous injection of melatonin prevented OVX-induced bone loss by inhibiting adipose tissue formation in the bone marrow.

3.2. *In vivo* treatment with melatonin preserved the differentiation balance of OVX-BMMSCs

To investigate the effect of melatonin on the differentiation equilibrium, we isolated BMMSCs from melatonin-treated OVX and sham rats and verified their differentiation potentials *in vitro*. BMMSCs derived from melatonin-treated and untreated OVX rats exhibited similar cell morphologies, while the proliferative capacity of the OVX + MT group was significantly higher than that of the OVX group (Fig. 5A&B). The mRNA expression level of *Sirt1* in BMMSCs from the melatonin-treated OVX rats was 88.8% higher than that of the OVX group (Fig. 5C). Meanwhile, compared to the OVX group, protein expression levels of SIRT1 and RUNX2 in the OVX + MT group were increased by 38.8% and 33.2%, respectively, while PPARγ expression levels were suppressed by 28.4% (Fig. 5D&E).

We further evaluated the osteogenic and adipogenic potentials of BMMSCs from melatonin-treated OVX rats. Matrix mineralization in the OVX + MT group was found to be 2.8-fold higher than in the OVX group (Fig. 5F&G) while transcript levels of osteoblast-specific markers were significantly up-regulated in the OVX + MT group (Supplementary Fig. 3A). In contrast, following adipogenic induction, levels of lipid formation in the OVX + MT group were 61.6% lower than those of the OVX group (Fig. 5H&I). In the OVX + MT group, gene expression levels of *Lpl* were down-regulated by 57.2%, *Pparg* by 54.7% and *Fabp4* by 43.5% compared to those of the OVX group (Supplementary Fig. 3B). These findings show that melatonin administration rescued the dysregulated lineage commitment of BMMSCs in OVX rats by favoring osteogenesis rather than adipogenesis.

4. Discussion

Increased marrow adiposity is correlated with progressive bone loss and increased facture risk in aged osteoporosis patients [30]. One putative cellular mechanism is that, with age, BMMSCs gradually lose their potential to differentiate into bone forming osteoblasts, while retaining their adipogenic differentiation capacity. The shift from osteogenic to adipogenic differentiation of BMMSCs results in impaired bone formation and elevated accumulation of marrow adipose tissues that eventually leads to osteoporosis [31]. However, the role of stem cell differentiation equilibrium in estrogen deficiency-induced osteoporosis was not established. We found that BMMSCs derived from OVX rats exhibited a dysregulated lineage commitment with an impaired osteogenic potential and an enhanced adipogenic differentiation. Significant increases in adipocyte numbers and marrow adipose tissue areas were confirmed in distal femurs of OVX rats. This is consistent with a recent study that reported a stronger adipogenic activity in BMMSCs derived from postmenopausal rats, accompanied with a low expression level of CXC chemokine receptor type 4 (CXCR4) and a reduced homing efficiency of BMMSCs [32]. Increased adipocytes in bone marrow negatively regulate bone metabolism and suppresse osteogenesis by releasing inflammatory cytokines (e.g. IL-1β, IL-6, and TNF-α) into bone marrow microenvironment [33]. Therefore, targeting the imbalance of osteogenesis and adipogenesis of BMMSCs is a promising way to improve bone formation during the development of osteoporosis.

Melatonin suppressed adipogenic and promoted osteogenic differentiations of OVX-BMMSCs in a dose-dependent manner. It was shown in Fig. 6 that activating SIRT1 signaling pathway regulated stem cell fate by inhibiting the PPARγ signaling pathway and activating the RUNX2 signaling pathway. In line with our findings, it has also been reported that melatonin directly inhibited adipogenic differentiation of normal human MSCs by suppressing PPARγ expression [19]. The nuclear receptor, PPARγ, is a master transcriptional regulator that induces adipogenic differentiation and promotes lipid storage and lipogenesis [34]. PPARγ binds the C/EBPα to recruit the expression of adipocyte-specific marker genes and activation of adipogenic signaling pathways [35]. Meanwhile, activation of PPARγ promotes cellular senescence by inducing p16INK4a expression, leading to the G0/G1 cell cycle arrest in human diploid fibroblasts [36]. Stimulatory effects of PPARγ on cellular senescence may also contribute to the shift of the balance between osteogenesis and adipogenesis in aged MSCs, as evidenced by the fact that adipogenic potential was better preserved over osteogenesis in MSCs subjected to extensive passages [37]. Melatonin treatment can effectively prevent replicative senescence and preserve the osteogenic potential of long-term passaged BMMSCs [38]. These findings show that regulation of PPARγ by melatonin may be a crucial factor in regulating lineage commitment of MSCs toward adipocytes or osteoblasts.

Studies have reported the advantages of melatonin on bone formation. Melatonin rescued the impaired osteogenic ability of OVX-BMMSCs by enhancing their intracellular antioxidant functions, particularly the activities of superoxide dismutase 2 (SOD2) [27]. Activation of ERK1/2 signaling cascade was proved to play a significant role in melatonin-facilitated *in vitro* osteogenesis of MSCs. Elevated levels of phosphorylated ERK1/2 have also been reported in bone tissues of mice that had been orally administrated with melatonin for one year [39]. Mechanistically, regulation of bone formation was possibly through the MT2 melatonin receptors. Knockout of MT2 rather than MT1 receptors in mice led to a decrease in bone mass without affecting bone resorption parameters. Osteoblasts isolated from MT2 knockout mice exhibited a cell intrinsic defect in osteogenic potential and mineralization abilities [40]. In addition, pro-inflammatory cytokines enhance osteoporosis by inhibiting osteoblast maturation and by promoting osteoclast-mediated bone resorption [41]. Melatonin is effective in rescuing pro-inflammatory cytokine-inhibited osteogenesis of human MSC, such as that of TNFα, possibly by decreasing SMURF1-mediated ubiquitination and subsequently stabilizing SMAD1 protein levels [18]. The direct inhibitory effect of melatonin on osteoclast differentiation has been reported in our previous study, in which melatonin suppressed Titanium nanoparticle-induced osteoclast activity via activation of the Nrf2/Catalase signaling pathway and successfully ameliorated periprosthetic osteolysis, a late complication of joint replacement [42]. More importantly, melatonin inhibits bone resorption via modulating the osteoblast functions. Maria et al. reported that, in layered cocultures of osteoblasts and osteoclasts, melatonin inhibited RANKL secretion from osteoblasts and thus suppressed osteoclast differentiation, suggesting that melatonin

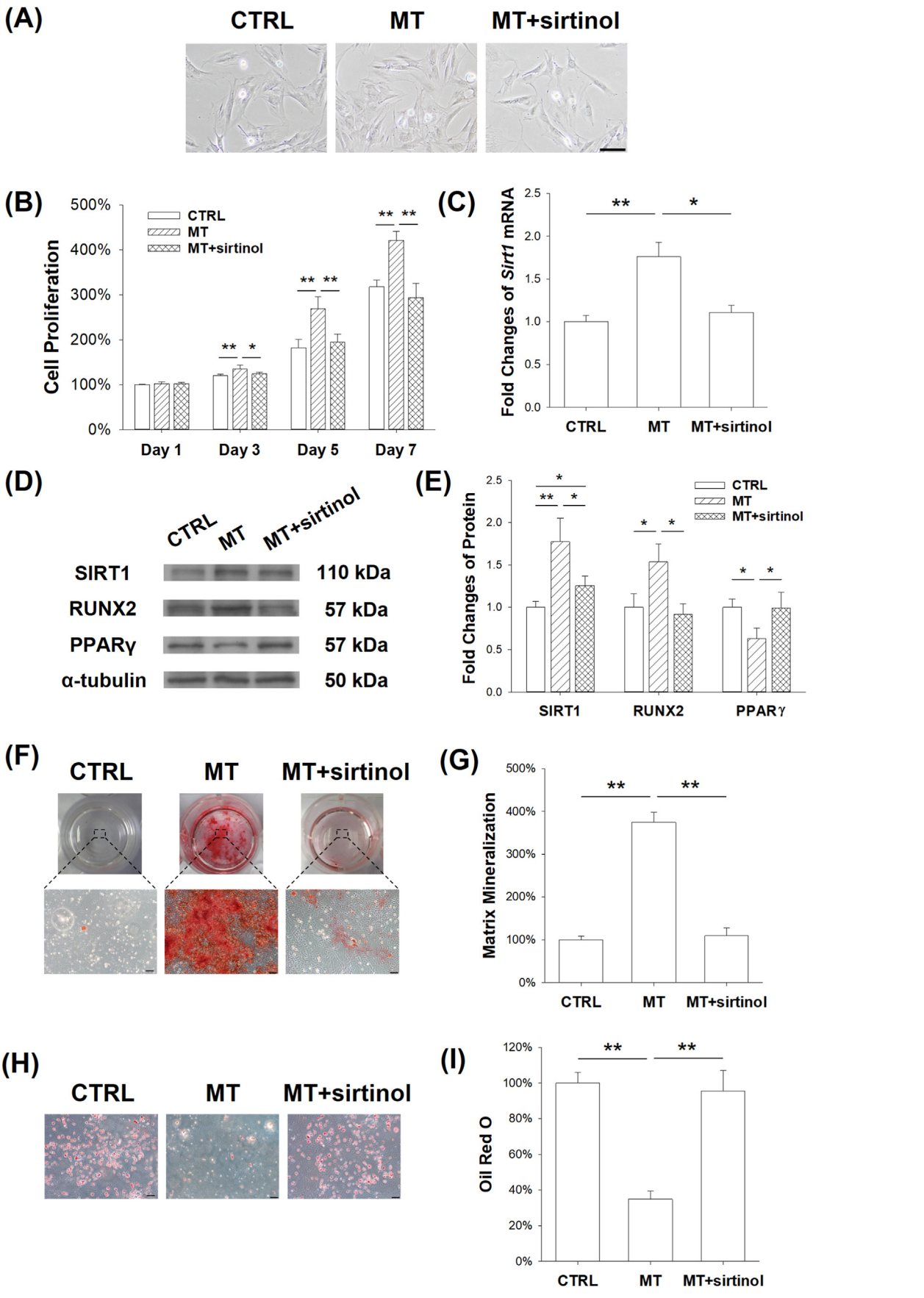

(caption on next page)

Fig. 3. Inurehibition of SIRT1 reversed melatonin-mediated effects on cell proliferation and stem cell lineage commitment (A) OVX-BMMSCs were treated with 40 μM sirtinol in the presence of 100 μM melatonin. Sirtinol treatment did not alter cell morphologies but suppressed cell densities of OVX-BMMSCs. Scale bar, 100 μm. Magnificantion, 100X. (B) Proliferation was suppressed by sirtinol treatment (C) Gene expression of Sirt1 in melatonin-treated OVX-BMMSCs were down-regulated by sirtinol treatment. (D–E) Protein expression levels of SIRT1, RUNX2 and PPARγ (F–G) OVX-BMMSCs were induced toward osteoblast differentiation with or without sirtinol. Matrix mineralization was evaluated by ARS staining. Scale bar, 100 μm. Magnificantion, 100X. (H–I) BMMSCs were induced toward adipogenesis with or without sirtinol. Lipid formation in mature adipocytes were determined by oil red O staining. Scale bar, 100 μm. Magnificantion, 100X. Values are the mean ± S.E.M of six independent experiments (n = 6) in cell proliferation assays, four independent experiments (n = 4) in RT-PCR experiments, ARS assays, and Oil Red O staining assays, and three independent experiments (n = 3) in Western blot assays. Statistically significant differences are indicated by * where $p < 0.05$ or ** where $p < 0.01$ between the indicated groups.
Abbreviations: MT, melatonin; SIRT1, Silent information regulator type 1; RUNX2, runt-related transcription factor 2; PPARγ, peroxisome proliferator-activated receptor γ.

may play an important role in regulating the interaction between bone formation and bone resorption [39].These findings show the potential therapeutic value of melatonin in prevention of estrogen deficiency-induced osteoporosis.

SIRT1, a key factor that regulates bone metabolism and determines stem cell fate of BMMSCs, is involved in melatonin-mediated anti-osteoporosis effects. Deficiency of SIRT1 in a mouse model of separation-based anorexia led to a significant decrease in bone mass and alteration of bone architecture, along with an obvious increase in bone marrow adiposity, whereas recovery of SIRT1 expression returned

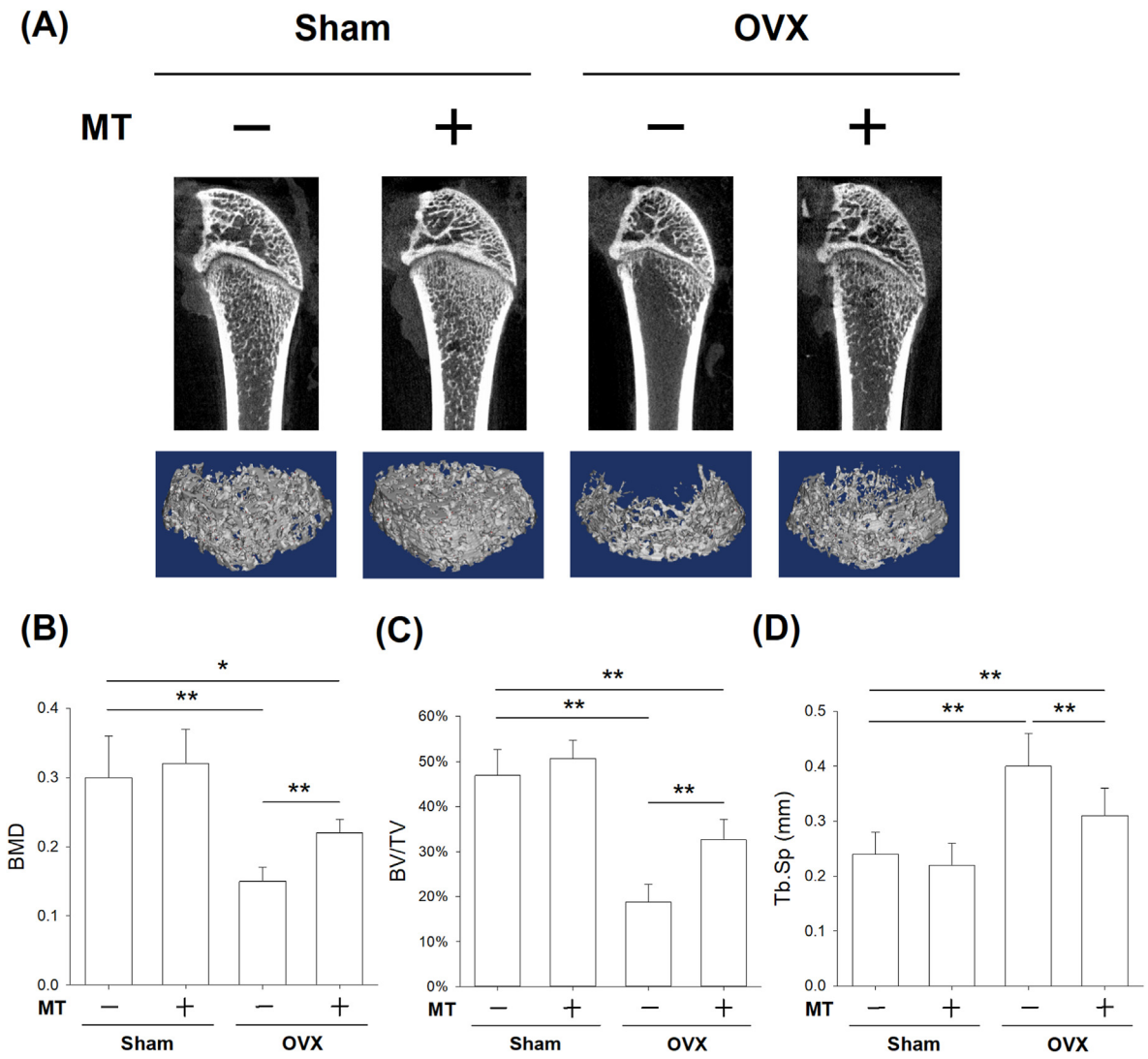

Fig. 4. Injection of melatonin ameliorated estrogen deficiency-induced bone loss and suppressed marrow fat accumulation in OVX rats. After ovariectomy, melatonin was injected into Sham or OVX rats through the tail vein (10 mg/kg). Rats administered with the same amount of ethanol served as controls (A) Representative μCT images of distal femurs of melatonin-treated and untreated rats. Effects of melatonin administration on BMD (B), BV/TV (C) and Tb.Sp (D) (E) Representative images of H&E staining of femoral sections from Sham and OVX with or without melatonin administration. Scale bar, 500 μm (upper panels), 200 μm (lower panels) (F) Representative images of oil red O staining of femoral sections that were used to label the marrow adipose tissue. (G) Number of adipocytes in the distal marrow per field view was quantified (H) Area of marrow adipose tissue was quantified. Values are the mean ± S.E.M of ten samples in each group (n = 10) in micro-CT and 3D reconstruction assays, and ten samples in each group (n = 10) in histological staining and oil red O staining *in vivo*. Statistically significant differences are indicated by * where $p < 0.05$ or ** where $p < 0.01$ between the indicated groups.
Abbreviations: OVX, ovariectomized; MT, melatonin; BMD, bone mineral density; BV/TV, bone volume ratio; Tb.Sp, trabecular separation.

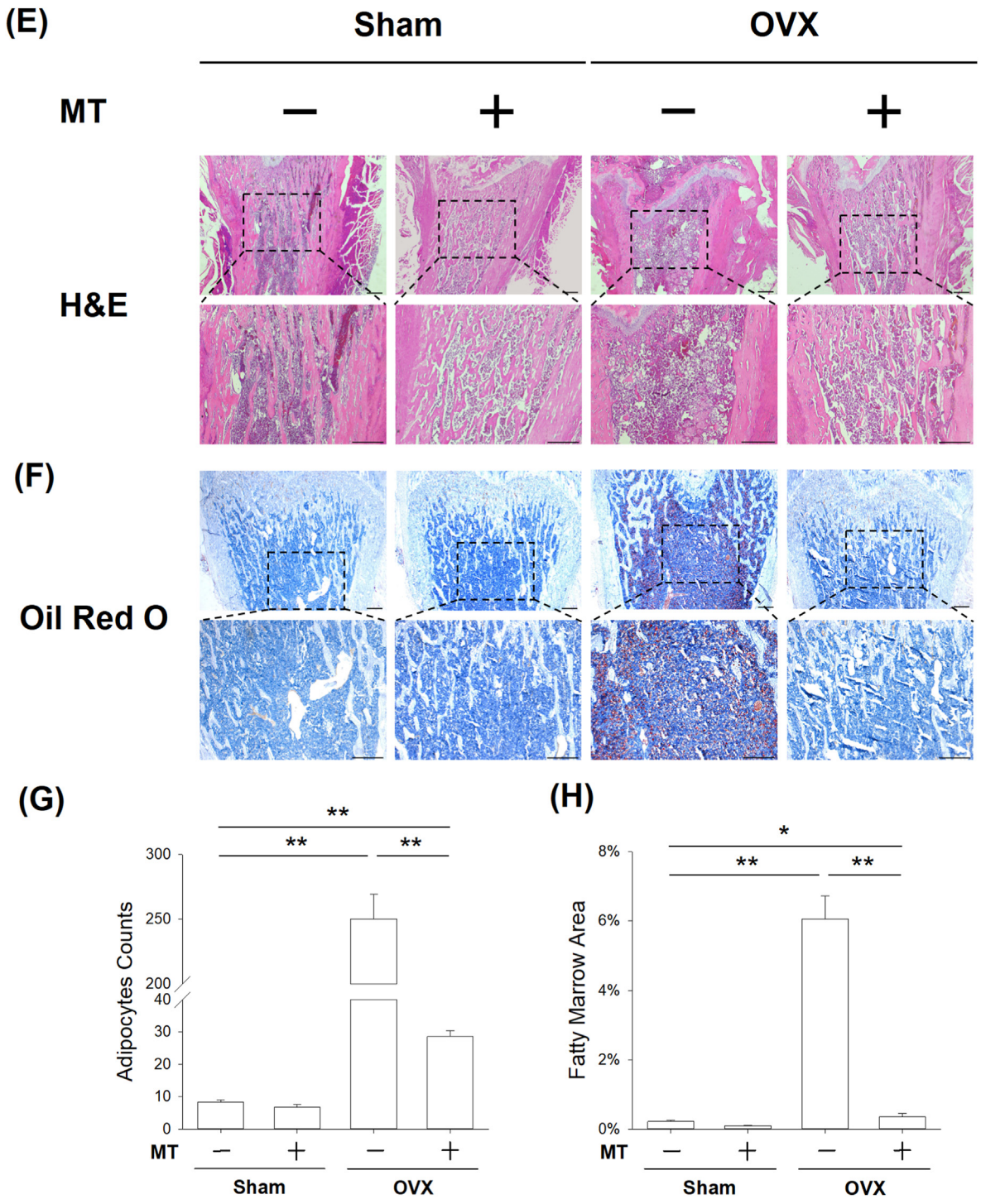

Fig. 4. (*continued*).

adiposity and bone mass to normal levels [43]. SIRT1 elevated the transcription activity of RUNX2 through its deacetylation activity and enhanced the expression of RUNX2-related osteogenic genes, while SIRT1 knockdown using antisense oligonucleotides induced Runx2 acetylation and suppressed osteoblast differentiation [44]. When SIRT1 interacts with forkhead box O3a (FOXO3A), the SIRT1-FOXO3A complex enhances RUNX2 promoter activity by binding to a distal FOXO response element. Activation of the SIRT1-FOXO3A axis modulates lineage commitment of MSCs to osteogenesis by up-regulating RUNX2 gene expression [24]. The decreased SIRT1 expression reduced deacetylation of RUNX2 and FOXO3A and thus inhibited their activity of suppressing adipogenesis. In addition to its deacetylation functions, SIRT1 promotes osteogenesis and bone formation via regulating intracellular antioxidant functions. Zhang et al. reported that melatonin-mediated activation of SIRT1 rescued titanium (Ti) wear particle-inhibited osteogenic differentiation of MSCs and protected mouse cranium from Ti particle-induced osteolysis [26]. Melatonin has also been shown to promote the expression and nuclear translocation of SIRT1 as well as the subsequent increase in SIRT1-mediated p53 deacetylation to protect mouse testes from palmitic acid-induced lipotoxicity and DNA damage [45].

In vivo experiments showed that intravenous injection of melatonin protected against estrogen deficiency-induced bone loss in OVX rats by

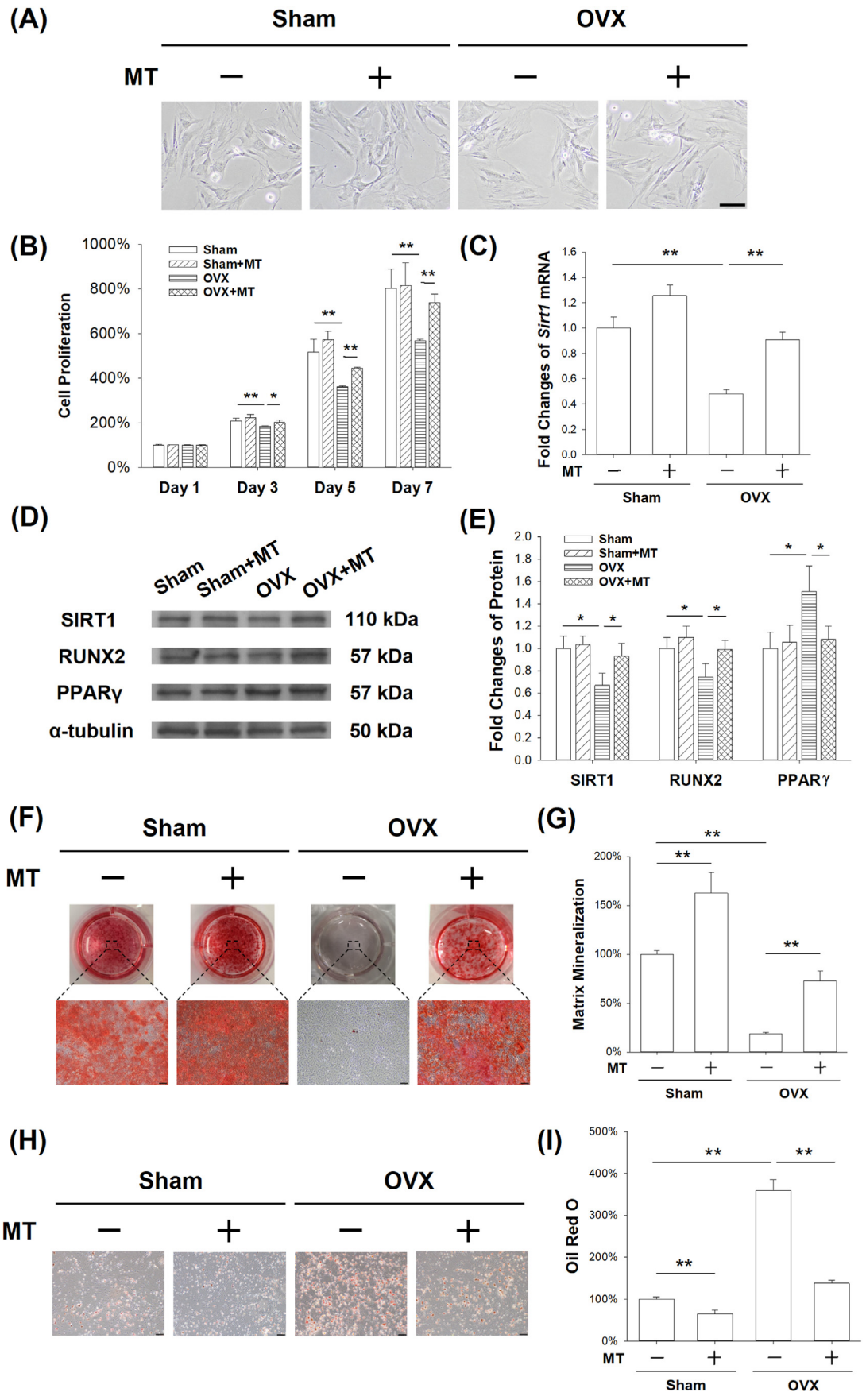

(caption on next page)

Fig. 5. Melatonin injection preserved osteogenic potential of BMMSCs in OVX rats while suppressing their adipogenic differentiation ability (A) BMMSCs were isolated from Sham and OVX rats with or without melatonin injection. BMMSCs exhibited similar cell morphologies. Scale bar, 100 μm. Magnificantion, 100X. (B) Proliferations of BMMSCs in OVX rats were increased by melatonin (C) Gene expression of Sirt1. (D–E) Protein expression of SIRT1, RUNX2 and PPARγ (F–G) BMMSCs from melatonin-treated or untreated rats were induced towards osteoblast differentiation. Matrix mineralization was evaluated by ARS staining. Scale bar, 100 μm. Magnificantion, 100X. (H–I) BMMSCs from melatonin-treated or untreated rats were induced toward adipogenesis. Lipid formation in mature adipocytes were determined by oil red O staining. Scale bar, 100 μm. Magnificantion, 100X. Values are the mean ± S.E.M of six independent experiments (n = 6) in cell proliferation assays, four independent experiments (n = 4) in RT-PCR experiments, ARS assays, and Oil Red O staining assays, and three independent experiments (n = 3) in Western blot assays. Statistically significant differences are indicated by * where $p < 0.05$ or ** where $p < 0.01$ between the indicated groups. Abbreviations: OVX, ovariectomized; MT, melatonin; SIRT1, Silent information regulator type 1; RUNX2, runt-related transcription factor 2; PPARγ, peroxisome proliferator-activated receptor γ.

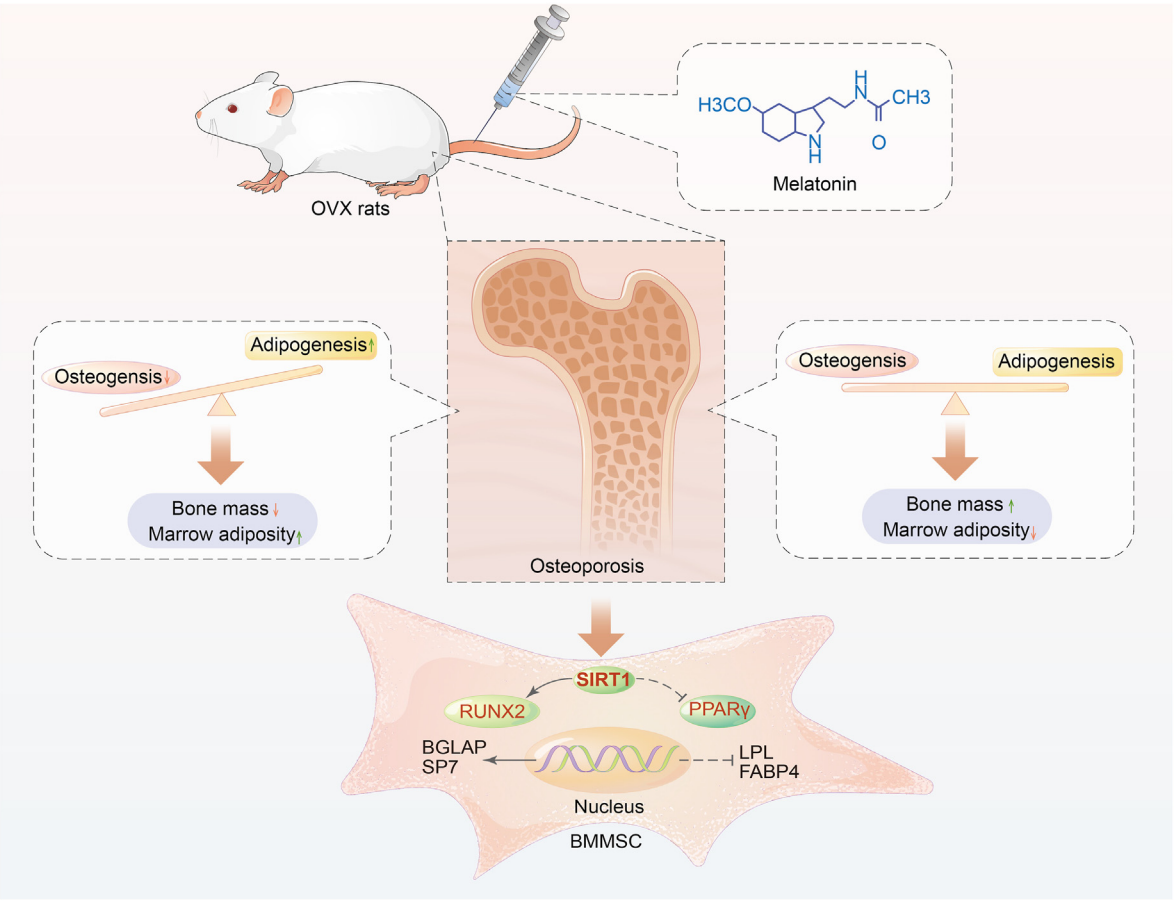

Fig. 6. A schematic diagram illustrating the underlying mechanism of melatonin-mediated anti-osteoporosis effect. BMMSCs derived from ovariectomized rats (OVX-BMMSCs) exhibit a lineage preference for adipocyte differentiation. *In vitro* treatment with melatonin enhances osteogenesis and suppresses adipogenesis of OVX-BMMSCs. *In vivo* administration of melatonin prevents bone mass loss and inhibits marrow adiposity. Activation of SIRT1 by melatonin is responsible for the restored equilibrium between osteogenesis and adipogenesis that promotes RUNX2 and down-regulates PPARγ.

preventing the over-accumulation of adipose tissues in the bone marrow. Consistent with our results, Qu et al. reported that overexpression of SIRT1 in MC3T3-E1 cells suppressed PPARγ expression and inhibited the adipogenic differentiation, whereas treatment with Rosiglitazone (an PPARγ agonist) reversed the inhibitory effect of SIRT1 on adipocyte formation by promoting the expression levels of FABP4 [46]. Qu et al. showed that reduction of SIRT1 was responsible for activation of PPARγ due to the increased acetylation activity and acetylated PPARγ further improved the transcription of its downstream molecules such as C/EBPα in MSCs [47]. During remodeling of white adipose tissue, SIRT1 deacetylates PPARγ on Lys293 and Lys268 to promote formation of the brown adipose tissue, implying that SIRT1-dependent PPARγ deacetylation plays a crucial role in modulating adipose production as well as insulin resistance [48]. Positive regulation of PPARγ by SIRT1 has been reported in a recently published study, in which fibroblast growth factor 19 (FGF19) promoted the expression of PPARγ in brown adipose tissues by activating SIRT1 and PGC-1α [49]. However, the exact mechanisms by which melatonin regulates SIRT1 and PPARγ during MSC lineage-specific differentiation have not been established. Considering the toxicity of sirtinol, *in vivo* experiments were not performed to investigate the effect of sirtinol on bone marrow adiposity in OVX rats. Future studies will focus on the role of SIRT1 in bone marrow fat accumulation using *Sirt1*$^{-/-}$ mice and liposomes will be used to load sirtinol to reduce its toxicity. Furthermore, biomaterials have been widely used in tissue engineering and regenerative medicine due to their biocompatibility and controllable drug delivery [50]. Future studies will be focused on the combination of melatonin and biomaterials to repair osteoporotic bone defects.

Increased bone marrow adiposity promotes osteoclast activity of bone resorption that is responsible for bone loss in postmenopausal osteoporosis. In the bone marrow of aged mice, pre-adipocytes expressing Pref-1 were found to secrete RANKL and were able to generate osteoclasts from

bone marrow macrophages. Early adipogenic transcription factors, C/EBPβ and C/EBPδ, in these cells stimulated RANKL gene expression by binding the RANKL promoter [51]. Yu et al. identified marrow adipogenic lineage precursors (MALPs) from the BMMSC population and showed that these adipocyte precursors promote osteoclastogenesis through expression of RANKL [52]. In addition, microRNAs, small non-coding RNAs that post-transcriptionally regulate gene expression, are involved in the regulation of osteoclast differentiation. Inhibition of miR-99a, which was found to be elevated during the initial stages of MSC adipogenic differentiation, promoted osteogenic differentiation and elevated osteoprotegerin (OPG) secretion to inhibit the formation of mature osteoclasts regulate [53]. However, it has not been established whether melatonin regulates osteoclast activity by suppressing the adipogenic differentiation of BMMSCs in the bone marrow. Regulatory mechanisms associated with the interactions between adipocytes and osteoclasts should be evaluated further. In this study, we injected melatonin via the tail vein of OVX rats. This method was similar to intravenous injection in clinical practice that is potentially effective considering the high bioavailability and short time to reach the maximal concentration. However, one of the limitations is lack of targeting effect. Since bisphosphonates is one of the bone-targeted radiopharmaceuticals, it can be used for developing lanthanide based radiolabeled hydroxyapatite nanoparticles (HAP NPs) by anchoring to the surface of polymers [54]. The present study also showed that no side effects were observed among melatonin-treated rats, indicating that administration of melatonin is safe to treat OP animals. Therefore, future studies will focus on the incorporation of melatonin with bisphosphonates to target osteocytes and osteoclasts.

5. Conclusion

Estrogen deficiency impaired the osteogenic potential of OVX-BMMSC, accompanied by an enhanced adipogenic differentiation. *In vitro* melatonin promoted osteogenic differentiation of OVX-BMMSCs by elevating RUNX2 levels, while suppressing adipogenic differentiation by suppressing PPARγ levels. Intravenous injection of melatonin prevented OVX-induced bone mass reduction and bone architecture destruction, and more importantly, inhibited adipose tissue formation in the bone marrow. As illustrated in Fig. 6, the SIRT1 signaling pathway played a key role in stem cell fate determination and in melatonin-mediated anti-osteoporosis effects. This study shows that by restoring the disturbed differentiation equilibrium between osteogenesis and adipogenesis of BMMSCs, melatonin is a promising therapeutic strategy to treat post-menopausal OP.

Credit authors statement

Xiaoxiong Huang: Data curation, Formal analysis. **Weikai Chen**: Data curation, Formal analysis. **Chao Gu**: Data curation, Formal analysis. **Hao Liu**: Formal analysis. **Mingzhuang Hou**: Data curation. **Wanjin Qin**: Data curation. **Xuesong Zhu**: Formal analysis, Methodology. **Xi Chen**: Funding acquisition, Investigation, Writing - original draft, review & editing. **Tao Liu**: Conceptualization, Funding acquisition, Investigation, Supervision, Writing - review & editing. **Huiling Yang**: Supervision, Writing - original draft, review & editing. **Fan He**: Conceptualization, Project administration, Supervision, Formal analysis, Funding acquisition, Writing - original draft, review & editing.

Data availability

The data that supports the findings of this study are available in the supplementary material of this article.

Funding

This study was supported by the National Natural Science Foundation of China (82072476, 82072410); Changzhou's Leading Talent Program of Changzhou Science and Technology Bureau (CQ20210121); the Natural Science Foundation of Jiangsu Province (BK20220046, BK20191173); the Priority Academic Program Development of Jiangsu Higher Education Institutions (PAPD).

Declaration of competing interest

The authors declare no conflict of interest.

Acknowledgement

We want to thanks for Home for Researchers editorial team (www.home-for-researchers.com) for their language editing services.

Appendix A. Supplementary data

Supplementary data to this article can be found online at https://doi.org/10.1016/j.jot.2022.10.002.

References

[1] Compston J, McClung M, Leslie WD. Osteoporosis. Lancet 2019;393:364–76.
[2] Hendrickx G, Boudin E, Van Hul W. A look behind the scenes: the risk and pathogenesis of primary osteoporosis. Nat Rev Rheumatol 2015;11:462–74.
[3] Reid IR. A broader strategy for osteoporosis interventions. Nat Rev Endocrinol 2020;16:333–9.
[4] Skjodt MK, Frost M, Abrahamsen B. Side effects of drugs for osteoporosis and metastatic bone disease. Br J Clin Pharmacol 2019;85:1063–71.
[5] Crane JL, Cao X. Bone marrow mesenchymal stem cells and TGF-beta signaling in bone remodeling. J Clin Invest 2014;124:466–72.
[6] Singh L, Brennan TA, Russell E, Kim JH, Chen Q, Brad Johnson F, et al. Aging alters bone-fat reciprocity by shifting in vivo mesenchymal precursor cell fate towards an adipogenic lineage. Bone 2016;85:29–36.
[7] Sui B, Hu C, Liao L, Chen Y, Zhang X, Fu X, et al. Mesenchymal progenitors in osteopenias of diverse pathologies: differential characteristics in the common shift from osteoblastogenesis to adipogenesis. Sci Rep 2016;6:30186.
[8] Knani L, Bartolini D, Kechiche S, Tortoioli C, Murdolo G, Moretti M, et al. Melatonin prevents cadmium-induced bone damage: first evidence on an improved osteogenic/adipogenic differentiation balance of mesenchymal stem cells as underlying mechanism. J Pineal Res 2019;67:e12597.
[9] Li T, Jiang S, Lu C, Yang W, Yang Z, Hu W, et al. Melatonin: another avenue for treating osteoporosis? J Pineal Res 2019;66:e12548.
[10] Igarashi-Migitaka J, Seki A, Ikegame M, Honda M, Sekiguchi T, Mishima H, et al. Oral administration of melatonin contained in drinking water increased bone strength in naturally aged mice. Acta Histochem 2020;122:151596.
[11] Egermann M, Gerhardt C, Barth A, Maestroni GJ, Schneider E, Alini M. Pinealectomy affects bone mineral density and structure–an experimental study in sheep. BMC Muscoskel Disord 2011;12:271.
[12] Amstrup AK, Sikjaer T, Heickendorff L, Mosekilde L, Rejnmark L. Melatonin improves bone mineral density at the femoral neck in postmenopausal women with osteopenia: a randomized controlled trial. J Pineal Res 2015;59:221–9.
[13] Kotlarczyk MP, Lassila HC, O'Neil CK, D'Amico F, Enderby LT, Witt-Enderby PA, et al. Melatonin osteoporosis prevention study (MOPS): a randomized, double-blind, placebo-controlled study examining the effects of melatonin on bone health and quality of life in perimenopausal women. J Pineal Res 2012;52:414–26.
[14] Zhou L, Chen X, Yan J, Li M, Liu T, Zhu C, et al. Melatonin at pharmacological concentrations suppresses osteoclastogenesis via the attenuation of intracellular ROS. Osteoporos Int 2017;28:3325–37.
[15] Ikegame M, Hattori A, Tabata M, Kitamura K, Tabuchi Y, Furusawa Y, et al. Melatonin is a potential drug for the prevention of bone loss during space flight. J Pineal Res 2019;67:e12594.
[16] Radio NM, Doctor JS, Witt-Enderby PA. Melatonin enhances alkaline phosphatase activity in differentiating human adult mesenchymal stem cells grown in osteogenic medium via MT2 melatonin receptors and the MEK/ERK (1/2) signaling cascade. J Pineal Res 2006;40:332–42.
[17] Liu X, Gong Y, Xiong K, Ye Y, Xiong Y, Zhuang Z, et al. Melatonin mediates protective effects on inflammatory response induced by interleukin-1 beta in human mesenchymal stem cells. J Pineal Res 2013;55:14–25.
[18] Lian C, Wu Z, Gao B, Peng Y, Liang A, Xu C, et al. Melatonin reversed tumor necrosis factor-alpha-inhibited osteogenesis of human mesenchymal stem cells by stabilizing SMAD1 protein. J Pineal Res 2016;61:317–27.
[19] Zhang L, Su P, Xu C, Chen C, Liang A, Du K, et al. Melatonin inhibits adipogenesis and enhances osteogenesis of human mesenchymal stem cells by suppressing PPARgamma expression and enhancing Runx2 expression. J Pineal Res 2010;49:364–72.
[20] Kato H, Tanaka G, Masuda S, Ogasawara J, Sakurai T, Kizaki T, et al. Melatonin promotes adipogenesis and mitochondrial biogenesis in 3T3-L1 preadipocytes. J Pineal Res 2015;59:267–75.

[21] Chen H, Liu X, Chen H, Cao J, Zhang L, Hu X, et al. Role of SIRT1 and AMPK in mesenchymal stem cells differentiation. Ageing Res Rev 2014;13:55–64.
[22] Wang H, Hu Z, Wu J, Mei Y, Zhang Q, Zhang H, et al. Sirt1 promotes osteogenic differentiation and increases alveolar bone mass via Bmi1 activation in mice. J Bone Miner Res 2019;34:1169–81.
[23] Simic P, Zainabadi K, Bell E, Sykes D, Saez B, Lotinun S, et al. SIRT1 regulates differentiation of mesenchymal stem cells by deacetylating β-catenin. EMBO Mol Med 2013;5:430–40.
[24] Tseng PC, Hou SM, Chen RJ, Peng HW, Hsieh CF, Kuo ML, et al. Resveratrol promotes osteogenesis of human mesenchymal stem cells by upregulating RUNX2 gene expression via the SIRT1/FOXO3A axis. J Bone Miner Res 2011;26:2552–63.
[25] Zhou L, Chen X, Liu T, Gong Y, Chen S, Pan G, et al. Melatonin reverses H_2O_2-induced premature senescence in mesenchymal stem cells via the SIRT1-dependent pathway. J Pineal Res 2015;59:190–205.
[26] Zhang Y, Zhu X, Wang G, Chen L, Yang H, He F, et al. Melatonin rescues the Ti particle-impaired osteogenic potential of bone marrow mesenchymal stem cells via the SIRT1/SOD2 signaling pathway. Calcif Tissue Int 2020;107:474–88.
[27] Chen W, Chen X, Chen AC, Shi Q, Pan G, Pei M, et al. Melatonin restores the osteoporosis-impaired osteogenic potential of bone marrow mesenchymal stem cells by preserving SIRT1-mediated intracellular antioxidant properties. Free Radic Biol Med 2020;146:92–106.
[28] Chen X, He F, Zhong D, Luo ZP. Acoustic-frequency vibratory stimulation regulates the balance between osteogenesis and adipogenesis of human bone marrow-derived mesenchymal stem cells. BioMed Res Int 2015;2015:540731.
[29] Bouxsein ML, Boyd SK, Christiansen BA, Guldberg RE, Jepsen KJ, Müller R. Guidelines for assessment of bone microstructure in rodents using micro-computed tomography. J Bone Miner Res 2010;25:1468–86.
[30] Ambrosi TH, Scialdone A, Graja A, Gohlke S, Jank AM, Bocian C, et al. Adipocyte accumulation in the bone marrow during obesity and aging impairs stem cell-based hematopoietic and bone regeneration. Cell Stem Cell 2017;20:771–784.e6.
[31] Tencerova M, Kassem M. The bone marrow-derived stromal cells: commitment and regulation of adipogenesis. Front Endocrinol 2016;7:127.
[32] Liu Q, Zhang X, Jiao Y, Liu X, Wang Y, Li SL, et al. In vitro cell behaviors of bone mesenchymal stem cells derived from normal and postmenopausal osteoporotic rats. Int J Mol Med 2018;41:669–78.
[33] Liu LF, Shen WJ, Ueno M, Patel S, Kraemer FB. Characterization of age-related gene expression profiling in bone marrow and epididymal adipocytes. BMC Genom 2011;12:212.
[34] Deng T, Sieglaff DH, Zhang A, Lyon CJ, Ayers SD, Cvoro A, et al. A peroxisome proliferator-activated receptor gamma PPARgamma coactivator 1beta autoregulatory loop in adipocyte mitochondrial function. J Biol Chem 2011;286:30723–31.
[35] Zhao Q, Wang S, Liu S, Li J, Zhang Y, Sun Z, et al. PPARγ forms a bridge between DNA methylation and histone acetylation at the C/EBPα gene promoter to regulate the balance between osteogenesis and adipogenesis of bone marrow stromal cells. FEBS J 2013;280:5801–14.
[36] Gan Q, Huang J, Zhou R, Niu J, Zhu X, Wang J, et al. PPAR(gamma) accelerates cellular senescence by inducing p16INK4(alpha) expression in human diploid fibroblasts. J Cell Sci 2008;121:2235–45.
[37] Yang YK, Ogando CR, See WC, Chang TY, Barabino GA. Changes in phenotype and differentiation potential of human mesenchymal stem cells aging in vitro. Stem Cell Res Ther 2018;9:131.
[38] Shuai Y, Liao L, Su X, Yu Y, Shao B, Jing H, et al. Melatonin treatment improves mesenchymal stem cells therapy by preserving stemness during long-term in vitro expansion. Theranostics 2016;6:1899–917.
[39] Maria S, Samsonraj RM, Munmun F, Glas J, Silvestros M, Kotlarczyk MP, et al. Biological effects of melatonin on osteoblast/osteoclast cocultures, bone, and quality of life: implications of a role for MT2 melatonin receptors, MEK1/2, and MEK5 in melatonin-mediated osteoblastogenesis. J Pineal Res 2018;64:e12465.
[40] Sharan K, Lewis K, Furukawa T, Yadav VK. Regulation of bone mass through pineal-derived melatonin-MT2 receptor pathway. J Pineal Res 2017;63:e12423.
[41] Rao SS, Hu Y, Xie PL, Cao J, Wang ZX, Liu JH, et al. Omentin-1 prevents inflammation-induced osteoporosis by downregulating the pro-inflammatory cytokines. Bone Res 2018;6:9.
[42] Zhu X, Zhang Y, Yang H, He F, Lin J. Melatonin suppresses Ti-particle-induced inflammatory osteolysis via activation of the Nrf2/Catalase signaling pathway. Int Immunopharm 2020;88:106847.
[43] Louvet L, Leterme D, Delplace S, Miellot F, Marchandise P, Gauthier V, et al. Sirtuin 1 deficiency decreases bone mass and increases bone marrow adiposity in a mouse model of chronic energy deficiency. Bone 2020;136:115361.
[44] Shakibaei M, Shayan P, Busch F, Aldinger C, Buhrmann C, Lueders C, et al. Resveratrol mediated modulation of Sirt-1/Runx2 promotes osteogenic differentiation of mesenchymal stem cells: potential role of Runx2 deacetylation. PLoS One 2012;7:e35712.
[45] Xu D, Liu L, Zhao Y, Yang L, Cheng J, Hua R, et al. Melatonin protects mouse testes from palmitic acid-induced lipotoxicity by attenuating oxidative stress and DNA damage in a SIRT1-dependent manner. J Pineal Res 2020;69:e12690.
[46] Qu B, Ma Y, Yan M, Gong K, Liang F, Deng S, et al. Sirtuin1 promotes osteogenic differentiation through downregulation of peroxisome proliferator-activated receptor γ in MC3T3-E1 cells. Biochem Biophys Res Commun 2016;478:439–45.
[47] Qu P, Wang L, Min Y, McKennett L, Keller JR, Lin CP. Vav1 regulates mesenchymal stem cell differentiation decision between adipocyte and chondrocyte via Sirt1. Stem Cell 2016;34:1934–46.
[48] Qiang L, Wang L, Kon N, Zhao W, Lee S, Zhang Y, et al. Brown remodeling of white adipose tissue by SirT1-dependent deacetylation of Pparγ. Cell 2012;150:620–32.
[49] Guo A, Li K, Tian HC, Fan Z, Chen QN, Yang YF, et al. FGF19 protects skeletal muscle against obesity-induced muscle atrophy, metabolic derangement and abnormal irisin levels via the AMPK/SIRT-1/PGC-α pathway. J Cell Mol Med 2021;25:3585–600.
[50] Wang W, Yeung KWK. Bone grafts and biomaterials substitutes for bone defect repair: a review. Bioact Mater 2017;2(4):224–47.
[51] Takeshita S, Fumoto T, Naoe Y, Ikeda K. Age-related marrow adipogenesis is linked to increased expression of RANKL. J Biol Chem 2014;289:16699–710.
[52] Yu W, Zhong L, Yao L, Wei Y, Gui T, Li Z, et al. Bone marrow adipogenic lineage precursors promote osteoclastogenesis in bone remodeling and pathologic bone loss. J Clin Invest 2021;131:e140214.
[53] Moura SS, Bras JP, Freitas J, Osório H, Barbosa MA, Santos SG, et al. miR-99a in bone homeostasis: regulating osteogenic lineage commitment and osteoclast differentiation. Bone 2020;134:115303.
[54] Lobaz V, Konefał R, Pánek J, Vlk M, Kozempel J, Petrík M, et al. In Situ In Vivo radiolabeling of polymer-coated hydroxyapatite nanoparticles to track their biodistribution in mice. Colloid Surface B 2019;179:143–52.